J. Chem. Sci. Vol. 126, No. 1, January 2014, pp. 265–272.

Theoretical studies on the mechanism of palladium(II)-catalysed *ortho*-carboxylation of acetanilide with CO

XING HUI ZHANG[a,*], ZHI YUAN GENG[b] and KE TAI WANG[a]

[a]College of Chemical Engineering, Lanzhou University of Arts and Science, Lanzhou, Gansu 730010, People's Republic of China

[b]Gansu Key Laboratory of Polymer Materials, College of Chemistry and Chemical Engineering, Northwest Normal University, Lanzhou, Gansu 730070, People's Republic of China

e-mail: zhxh135@126.com

MS received 28 July 2013; revised 23 September 2013; accepted 25 September 2013

Abstract. The mechanism of palladium(II)-catalysed carboxylation of acetanilide with CO has been investigated using density functional theory calculation done at the B3LYP/6-31G(d, p)(SDD for Pd) level of theory. Solvent effects on these reactions have been explored by calculation that included a polarizable continuum model (PCM) for the solvent. Two plausible pathways which led to the formation of anhydride or benzoxazinone intermediate structure were proposed. Our calculated results suggested that the steps of forming the anhydride or benzoxazinone intermediate became the rate-determining one in the whole catalytic cycle. The process of forming benzoxazinone is more favoured kinetically with a barrier of 16.6 kcal/mol versus 22.9 kcal/mol for the pathway of forming anhydride structure. Subsequent hydrolysis process of these intermediates then provide the corresponding product *ortho*-acetaminobenzoic acid. The computational results are consistent with the experimental observations of Yu *et al.* for palladium(II)-catalysed synthesis of acetanilide based on carbon monoxide.

Keywords. Carboxylation; palladium(II)-catalysed; acetanilide; C-H activation; density functional theory.

1. Introduction

Carbonylation of organic compounds is an expedient route and an attractive synthetic process to access carboxylic acid derivatives and develop transition-metal catalysts.[1] Ar-H and Ar-FG (FG=functional group) utilize carbon monoxide as a carbon source for the formation of functionalized aromatic rings with a new C-C bond. Carbonylation reactions of vinyl halides, aryl halides, mesylates, triflates, fluorosulphonates and tosylates with CO have been explored to produce carboxylic acids, amides and esters[2–13] since the study was reported by Heck in 1974.[14,15] As we know, many efficient transition-metal catalysts have been found for carbonylation.[16–20] In particular, palladium-catalysed C-H activation has long been recognized as being difficult and requiring high temperatures for carbonylation using CO.[21] However, recently there was an experimental report for palladium (II)-catalysed carboxylation of C-H bond activation in acetanilide with CO to form *ortho*-acetaminobenzoic acid by the Yu and Giri group (see scheme 1).[22,23] Carboxylation of palladium (II)-catalysed, it has been reported that

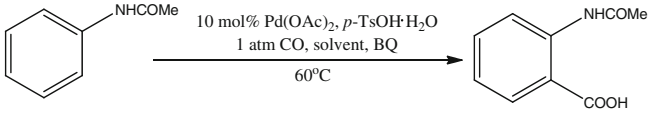

Scheme 1. Palladium(II)-catalysed carboxylation of acetanilide via *ortho*-C-H activation.

p-toluenesulphonic acid (*p*-TsOH) plays a crucial role in assisting in the cleavage of acetanilide *ortho*-C-H bond, by Lloyd-Jones and co-workers.[13]

According to the experimental results, two general mechanisms were postulated to explain the formation of *ortho*-acetaminobenzoic acid from acetanilide. As depicted in scheme 2, the first step, acetanilide with $Pd(OAc)_2$ in the presence of *p*-TsOH·H_2O gave a cyclopalladated intermediate **A**. **A** subsequently would be inserted CO to generate palladacycle **B**, which then undergoes reductive elimination with *p*-toluenesulphonate to give a mixed anhydride species **D** (scheme 2, path A). Alternatively, intermediate **B** could release a molecule of *p*-TsOH via enolization of the acidic N-H bond to generate a second intermediate **C**, which subsequently undergoes reductive elimination to generate benzoxazinone **E** (scheme 2, path B). The final mixed anhydride **D** and benzoxazinone **E**

*For correspondence

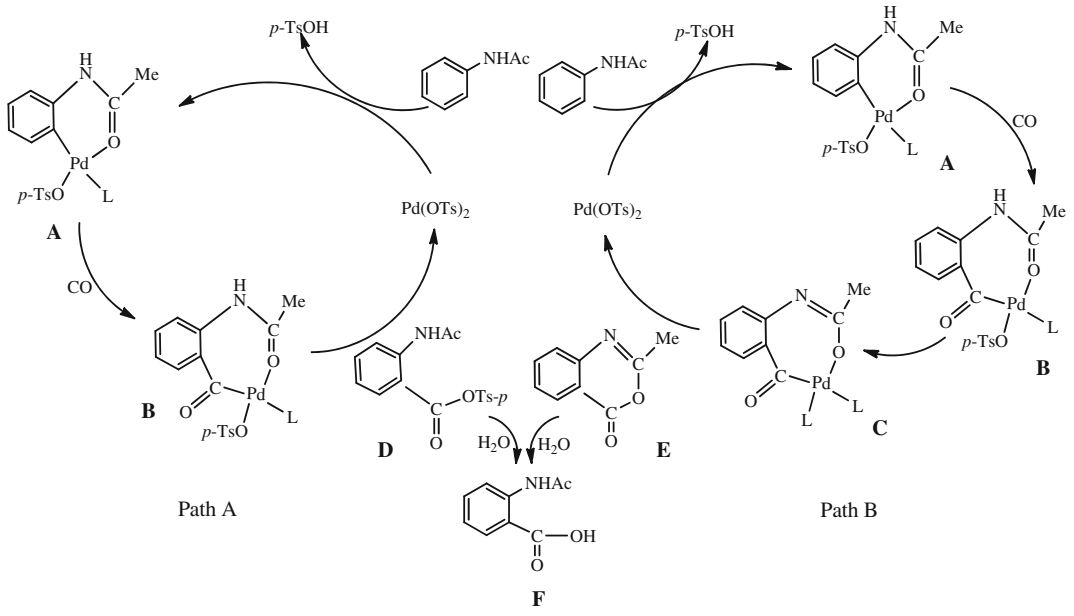

Scheme 2. Dual-reaction pathways of catalytic carboxylation in the presence of H_2O.

provides the corresponding carboxylic acid product **F** in the water-present reaction system.

To our knowledge, there are no detailed theoretical studies on the novel palladium (II)-catalysed transformation, reported by Yu *et al.*[22] Here, we present a detailed density functional theory (DFT) computational investigation of the mechanism of palladium (II)-catalysed carboxylation of acetanilide to give the corresponding *ortho*-acetaminobenzoic acid on the basis of experimental evidence reported by Yu and coworkers.[22] A plausible and more detailed mechanism was proposed for this novel palladium(II)-catalysed carboxylation as shown in scheme 3. The geometries of the possible intermediates involved in the reaction pathways are based on those suggested in the literature. The present DFT study located the transition states for the reactions of interest and performed a vibrational analysis at these stationary points. From the results shown here, we attempt to gain a more detailed understanding of the catalytic mechanism and find out more about the factors that control the activation barriers of the reaction systems, and further investigate the effects of solvent on the thermodynamic and kinetic properties of this reaction.

2. Computational methods

The geometries of all the structures were fully optimized by hybrid DFT method[24] at the B3LYP level[25] using the GAUSSIAN 03 program suite.[26] This hybrid DFT method has been successfully applied in the mechanistic studies of transition-metal- or non-transition-metal-catalysed reactions.[27–29] The 6-31G basis set with polarization (d and p)[30] was selected for all of the atoms except palladium, for which the Stuttgart–Dresden effective core potential[31] was employed to account for relativistic effects and to substantially reduce the number of electrons in the system.[32] Analytical frequency calculations at the same level have also been performed to confirm all the stationary points to be either an intermediate or a transition structure as well as to obtain the zero-point energy correction. Relative energies were thus corrected for the vibrational zero-point energies (ZPE, not scaled). Intrinsic reaction coordinate (IRC) calculations[33] for the transition state models were calculated in order to further verify that transition structures indeed connect relevant reactants, products, and intermediates in several significant cases. In consideration of the solvent effects on the reactions of interest, we applied a continuum medium to do single-point salvation energy calculations for all of the species calculated along the minimum energy pathway, using UAHF radii on the polarizable continuum model (PCM).[34,35] The PCM calculations were done at the B3LYP/PCM/6-311++G(d, p)// B3LYP/6-31G(d, p) (SDD for Pd) level of theory. TFA was used as the solvent, corresponding to the experimental conditions.

3. Results and discussion

Energy profiles for the two different reaction pathways of the catalytic cycles are shown in figure 1. Optimized

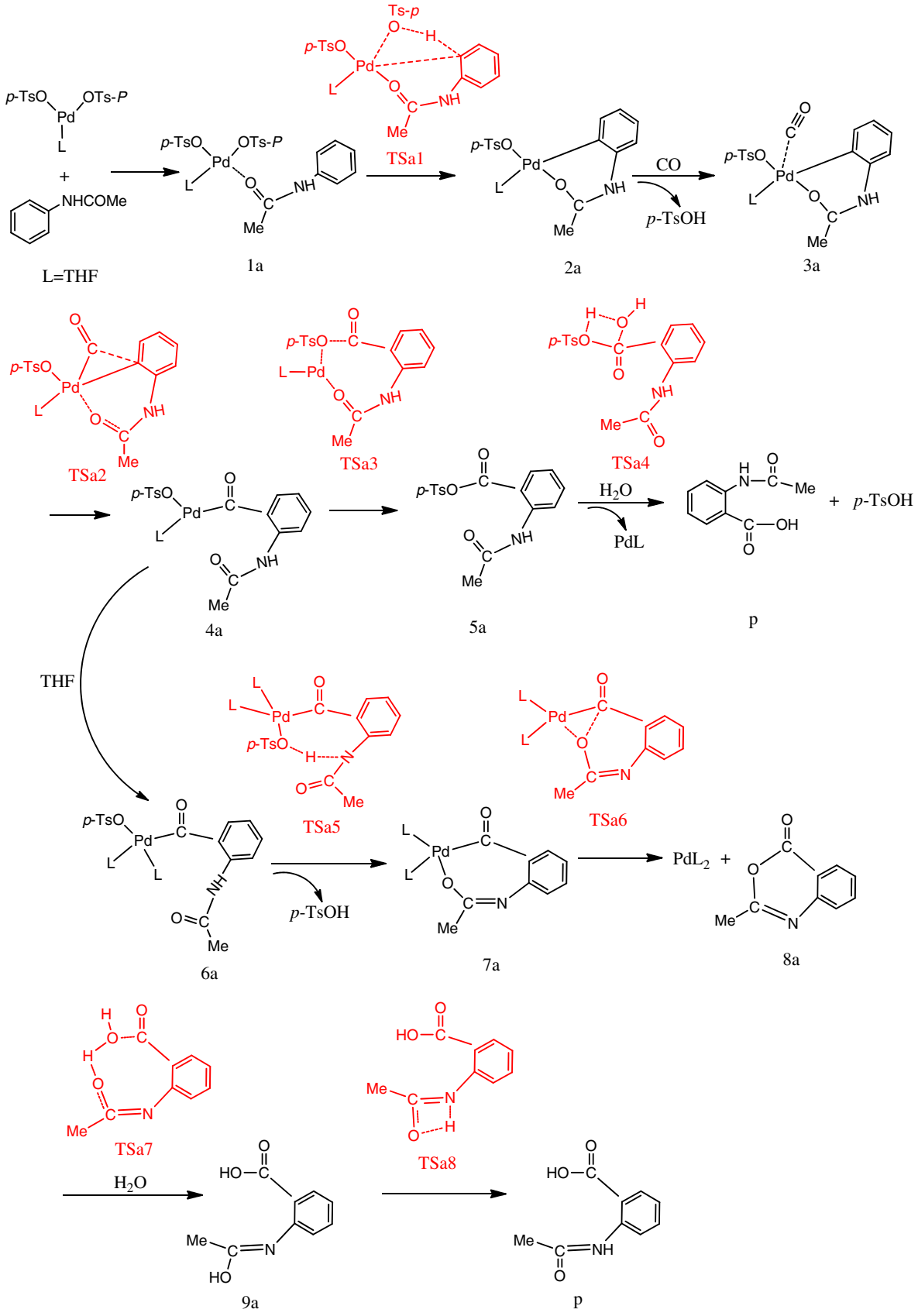

Scheme 3. Two plausible and more detailed mechanisms were proposed for this novel palladium(II)-catalysed carboxylation.

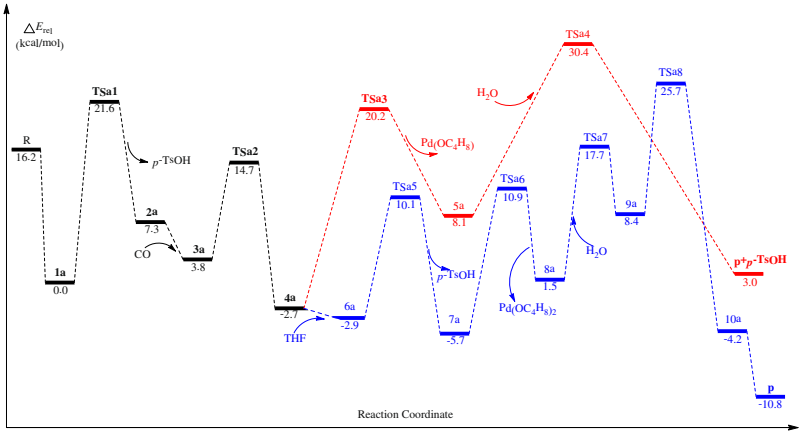

Figure 1. Potential energy surface of the carboxylation for acetanilide with CO catalysed by palladium(II) complexes (pathway a in red and pathway b in blue). Relative energies are given in kcal/mol.

geometries for the reactants [R = acetanilide + (p-TsO)$_2$Pd(OC$_4$H$_8$)], intermediates, transition states, and products of the reaction systems are depicted schematically in figure 2 along with selected key geometry parameters (e.g., bond lengths). Relative energies in the gas and solution phases are shown in table 1. Unless otherwise noted, the relative energies discussed in subsequent sections refer to the value in TFA solvent. In order to keep the computational cost low, the original (p-TsO)$_2$Pd(OC$_4$H$_8$) was selected with palladium's ligand p-TsO- replaced with C$_6$H$_4$SO$_3$- group as a model.

3.1 *Pathway a: Palladium(II)-catalysed carboxylation of acetanilide with CO to anhydride intermediate*

Free energy profile for pathway a is represented in figure 1. Structures of the various critical points located on the potential surface along with the values of the most relevant geometry parameters are shown in figure 2. As we know, the oxygen atom of carbonyl group is characterized by stronger electronegativity, which is higher in energy and easily interacts with the d orbitals in transition metals (electrophiles). Thus, from the energy profile, it is evident that the first step of the pathway indeed involves the preliminary intermediate 1a stabilized by the interaction of the carbonyl group of acetanilide with the palladium atom. If we consider (p-TsO)$_2$Pd(OC$_4$H$_8$) as the 'active' species of the catalyst, **1a** forms without any barrier and is 16.2 kcal/mol lower in energy than the reactants [R=(p-TsO)$_2$Pd(OC$_4$H$_8$)+ acetanilide]. In **1a**, the length of the new Pd-O^1 bond is 2.066 Å; the C^1-O^1 bond has lost a small amount of its C=O double-bond character and is now 1.258 Å (1.223 Å in R). Meanwhile, the Pd-O^3 and Pd-O^4 bonds have undergone little change from 2.032 and 1.970 Å (in **R**) to 2.021 and 2.020 Å, respectively. In **1a**, the coordination of the C=O double bond with the palladium atom enhances the activity of *ortho*-C-H of acetanilide. The new and stable intermediate **2a** is formed through the hydrogen atom shift transition structure **TSa1**. (**TSa1** has only one imaginary frequency of 163.7 i cm^{-1} and IRC calculations confirmed that this TS connects the corresponding reactants and intermediate.) Inspection of figure 2 shows that palladium atom is completely connected with C^3 atom of acetanilide (Pd-C^3 bond distance is 2.111 Å) in **TSa1**. Furthermore, bonds of C^3−H^1 and O^3−H^1 atoms are 1.221 to 1.506 Å, respectively. The transition vector obtained from the frequency computations on **TSa1** is dominated by the C^3−H^1 and O^3−H^1 distances. These changes in the bond lengths are attributed to partial formation of the p-TsOH molecule in **TS1a**. Inspection of table 1 shows that the energy of activation for this step is calculated to be 21.6 kcal/mol for **TSa1** and the energy of reaction for the **2a** intermediate and p-TsOH is 7.3 kcal/mol with respect to **1a**. In **2a**, it is evident that the intermediate including six-membered ring structures is also found and the Pd-C^3 becomes completely formed (1.980 Å). A subsequent step for the palladium atom of **2a** is attacked via carbon atom of CO to form the intermediate **3a**. The new Pd-C^2 bond length is 2.973 Å in **3a** and **3a** is 3.5 kcal/mol lower in energy than **2a** +CO. Due to the ring strain of the six-membered ring, structure **3a** is then converted to the seven-membered ring intermediate **4a** via the CO insertion transition structure **TSa2**. In **TSa2**, the breaking Pd-O^1 and Pd-C^3

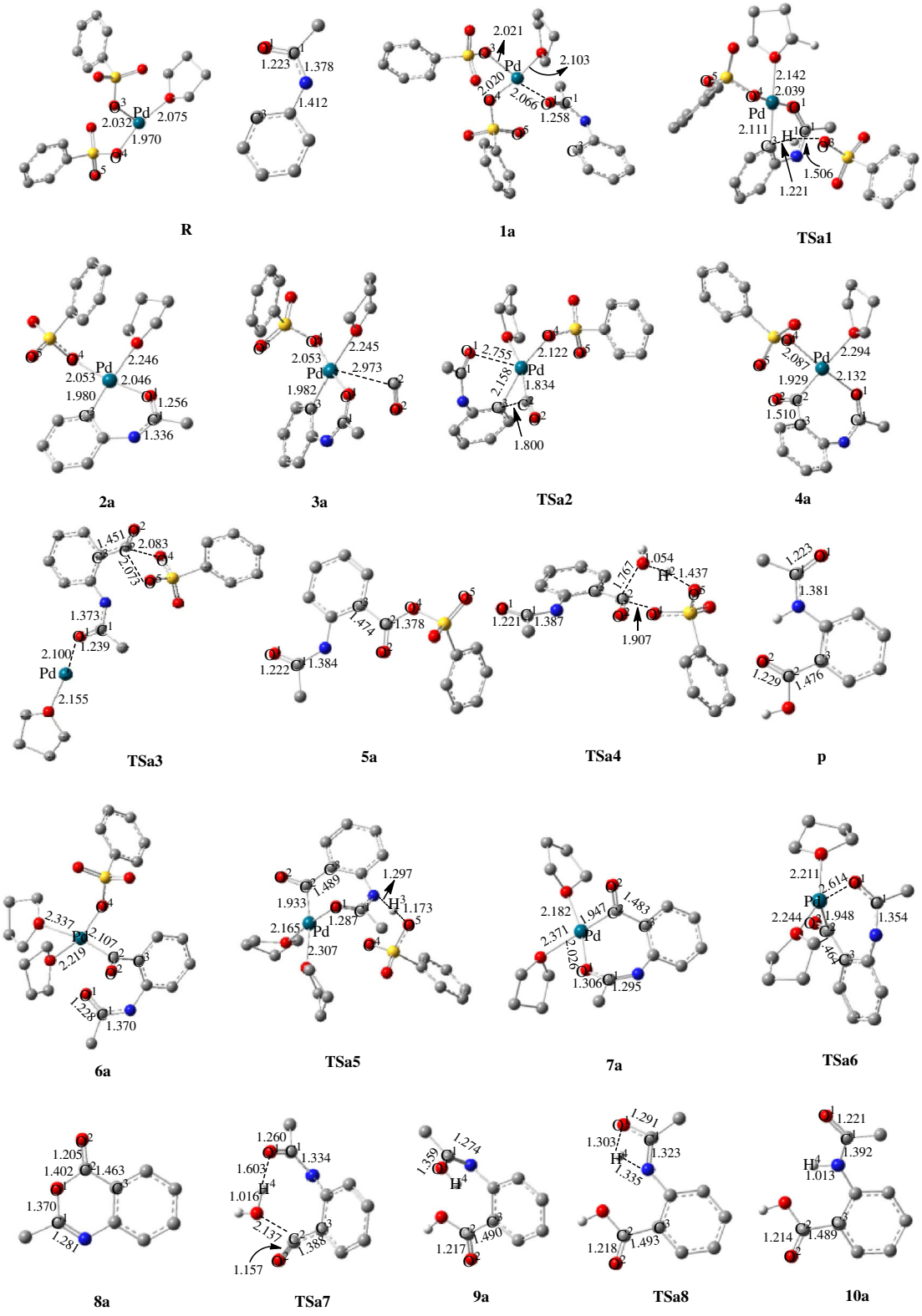

Figure 2. Optimized geometries for the species shown in figure 1, with selected structural parameters (bond lengths in Å). For the sake of clarity, the H atoms in structures are omitted (except for the H atoms that formed hydrogen bonds).

bonds are 2.755 and 2.158 Å, respectively. Meanwhile, the lengths of the two new formed Pd-C2 and C3-C2 bonds are 1.834 and 1.800 Å, respectively. Activation energy of the second step is 10.9 kcal/mol, and the formation of **4a** is an exergonic process (energy of reaction for **4a** is −6.5 kcal/mol with respect to **3a**).

Table 1. Thermodynamic properties (total energies and relative energies in the gas phase and in solution) of the structures in figure 1.

Species	E_{ZPE}(a.u.)	Et_{gas} (a.u.)	Er_{gas} (kcal/mol)	Et_{sol}(a.u.)	Er_{sol} (kcal/mol)	$\Delta E_{sol}^{\neq}$ (kcal/mol)
R	0.48530	−2511.10119	17.0	−2512.09815	16.2	
1a	0.48803	−2511.12833	0.0	−2512.12396	0.0	0.0
TSa1	0.48257	−2511.10102	17.1	−2512.08950	21.6	21.6
2a+***p*-TsOH**	0.48517	−2511.11868	6.1	−2512.11236	7.3	
2a+CO	0.37551	−1768.48466	6.1	−1769.25035	7.3	
3a	0.37595	−1768.48654	4.9	−1769.25593	3.8	
TSa2	0.37603	−1768.47951	9.3	−1769.23859	14.7	10.9
4a	0.37929	−1768.50370	−5.8	−1769.26636	−2.7	
TSa3	0.37793	−1768.46289	19.8	−1769.22980	20.2	22.9
5a+Pd(OC_4H_8)	0.37901	−1768.48123	8.3	−1769.24910	8.1	
5a+H_2O	0.28245	−1484.61627	8.3	−1485.24539	8.1	
TSa4	0.28447	−1484.58463	28.2	−1485.20983	30.4	22.3
p+*p*-TsOH	0.28569	−1484.63209	−1.6	−1485.25350	3.0	
4a+THF	0.49620	−2000.84708	−5.8	−2001.78964	−2.7	
6a	0.49774	−2000.84790	−6.3	−2001.78990	−2.9	
TSa5	0.49347	−2000.83002	4.9	−2001.76930	10.1	13.0
7a+*p*-TsOH	0.49480	−2000.84856	−6.7	−2001.79439	−5.7	
7a	0.38011	−1144.87922	−6.7	−1145.53361	−5.7	
TSa6	0.37889	−1144.84630	14.0	−1145.50713	10.9	16.6
8a+Pd(OC_4H_8)$_2$	0.38056	−1144.87478	−3.9	−1145.52213	1.5	
8a+H_2O	0.16496	−628.66265	−3.9	−629.02212	1.5	
TSa7	0.16503	−628.63535	13.2	−628.99634	17.7	16.2
9a	0.16985	−628.66161	−3.2	−629.01113	8.4	
TSa8	0.16525	−628.63427	13.9	−628.98356	25.7	17.3
10a	0.17096	−628.67930	−14.3	−629.03124	−4.2	
p	0.17100	−628.69366	−23.4	−629.04172	−10.8	

The intermediate **4a** is a very crucial structure for two reaction channels (pathway a in red and pathway b in blue). In **4a**, the Pd-O^1, Pd-C^2 and C^2-C^3 bond lengths are computed to be 2.131, 1.929 and 1.510 Å, respectively. For pathway a, the intermediate **4a** then occurs the Pd-C^2 bond-breaking and TsO group shift to give the intermediate **5a** and regeneration of the catalyst ($PdOC_4H_8$) via the transition structure **TSa3**. Examination of figure 2 shows that the bonds of Pd–O^1,C^2-O^4 and C^2-O^5 are 2.100, 2.083 and 2.073 Å in **TS5a**, respectively.

Activation energy of this step is 22.9 kcal/mol and the formation of **5a** is an endothermic process (free energy of reaction for the **5a** is 10.8 kcal/mol with respect to **4a**). Higher barrier found for the step shows that this step is also the rate-determining one for the whole catalytic process of the pathway a. The final step is hydrolysis process for the intermediate **5a** leading to the formation of the final product (**p**) and *p*-TsOH through **TSa4**. Table 1 shows that the final barrier of 22.3 kcal/mol is required to release the products and the final step is exothermic by −5.1 kcal/mol. In total, the whole catalytic process is exothermic by −13.2 kcal/mol lower than the reactants (**R**).

3.2 *Pathway b: Palladium(II)-catalysed carboxylation of acetanilide with CO to benzoxazinone intermediate*

Changing the different ligands of palladium complex would give rise to another possible reaction pathway. The energy profile for this process is depicted in figure 1. The structures of the various critical points located on the potential energy surface along with the values of the most relevant geometry parameters are presented in figure 2. Examination of figure 1 shows that the reaction pathway b has the same reaction process in the early stage as the reaction pathway a, generating intermediate **4a**. It is evident that the first step for pathway b forms a new intermediate (**6a**) when the THF and **4a** structure move each other, where the oxygen atom of THF attacks the palladium atom of the intermediate **4a**. The step takes place without any barrier and is 0.2 kcal/mol lower than **4a**. In **6a**, the palladium atom is completely broken with the O^1 atom and the palladium atom is completely connected with the O atom of THF. Furthermore, bonds of Pd-C^2 and Pd-O^1 change from 1.929 to 2.107 Å and from 2.132 to 2.958 Å, respectively. The structure **6a** can also undergo

a hydrogen shift to give the intermediate structure **7a** and release the *p*-TsOH molecule through seven-membered ring transition structures **TSa5**. Inspection of figure 2 shows that bond distances N-H^3 and O^5-H^3 are 1.297 and 1.173 Å, and the bond of Pd-O^1 has formed (2.078 Å) in **TSa5**. Table 1 shows that activation energy of this step is 13.0 kcal/mol and reaction energy for **7a** is −2.8 kcal/mol with respect to **6a**.

From **7a** to **8a** is a bond dissociation process and regeneration of the catalyst [$Pd(OC_4H_8)_2$] through the transition structure **TSa7**, and the bond of the Pd-O^1 changes from 1.947(**7a**) to 2.614 Å (**TSa6**). Activation energy of the step is 16.6 kcal/mol, and the formation of **8a** is an endothermic process (energy of reaction for the **8a** is 7.2 kcal/mol with respect to **7a**). The subsequent step for the benzoxazinone intermediate **8a** is prone to hydrolysis reaction to **9a** in the presence of water via **TSa7**. Figure 2 shows that the bond lengths O^1-H^4, H^4-O(H_2O) and C^2-O(H_2O) are 1.603, 1.016 and 2.137 Å in **TSa7**, respectively. Table 1 and figure 1 show that the energy of activation for **TSa7** is calculated to be 16.2 kcal/mol. The next step for hydrogen migration of **9a** results in the formation of the intermediate **10a** through **TSa8**, and subsequent isomerization of the intermediate **10a** generates the final product **p**. The reaction for the final step has a barrier of 17.3 kcal/mol and is exothermic by about 19.2 kcal/mol, and the whole catalytic process is exothermic by −27.0 kcal/mol lower than the reactants. It is important to point out that this step is also the rate-determining step due to higher barriers found for **TS8a**. Relatively high barriers are found for the pathway a of 22.9 kcal/mol. However, barriers for pathway b stayed relatively lower. Consequently, reaction for the pathway b occurs more easily.

3.3 *General reactivity: anhydride intermediate structure vs benzoxazinone intermediate structure*

Previous experimental reports speculated that the formation of palladacycle structure as **B** (scheme 2) of palladium(II)-catalysed carboxylation of acetanilide with CO might take place by insertion of CO into the *ortho*-C-Pd bond of intermediate **A**. According to experimental results, two plausible mechanisms have been postulated to explain the formation of palladium(II)-catalysed carboxylation from **B**. Our calculations provided a palladacycle structure **4a** instead of the intermediate **B** proposed by Yu and co-workers in scheme 2.[22] As we know, the actual pathway that is followed to reach **5a** or **8a** is determined by the energy difference between the transition states of highest energy along the different pathways. According to our calculated results, **TSa3** and **TSa6** play vital roles in the title reaction. Higher activation energy found for **TSa3** indicates that the formation of the anhydride intermediate structure **5a** from **4a** via a TsO group migration should be unfavourable. However, the relative energy difference between the activation energies of **TSa6** is 16.6 kcal/mol, which suggests that the major pathway of the cycle causes an oxygen atom shift of carbonyl group and regenerates the catalyst leading to a benzoxazinone intermediate **8a**. Subsequent hydrolysis process of the intermediates **5a** and **8a** then provides the corresponding product **p** (**F** in scheme 2). Our calculated results are in good agreement with the experimental observations of Yu *et al.*[22]

4. Conclusion

In summary, this research has provided the first theoretical study for the reaction of the palladium(II)-catalysed *ortho*-carboxylation of acetanilide with CO. The calculated results indicate that the major step of the cycle involves a palladacycle intermediate structure for two possible pathways. Subsequently, the reaction proceeds through two different channels, and the formation of anhydride intermediate structure or benzoxazinone intermediate structure is the rate-determining step of two pathways, respectively. According to our calculations, the major pathway of the cycle should involve an oxygen atom shift of carbonyl group and regenerates the catalyst to form a benzoxazinone intermediate structure. The final hydrolysis process of this intermediate then provides the corresponding product *ortho*-acetaminobenzoic acid. However, the pathway including anhydride intermediate structure has the higher activation energy. Our computational results are in good agreement with the experimental observations of Yu *et al.*[22] for palladium(II)-catalysed carboxylation of acetanilide based on carbon monoxide.

Acknowledgements

This work was supported by the Natural Science Foundation of Department of Education, Gansu Province (1013B-01), and the Natural Science Foundation of Gansu Lianhe University (2012GGTS02). We thank the Gansu Province Supercomputer Center for essential support.

References

1. Munday R H, Martinelli J R and Buchwald S L 2008 *J. Am. Chem. Soc.* **130** 2754

2. Barnard C F J 2008 *Organometallics* **27** 5402
3. Yu W Y, Sit W N, Lai K M, Zhou Z and Chan A S C 2008 *J. Am. Chem. Soc.* **130** 3304
4. Dick A R and Sanford M S 2006 *Tetrahedron* **62** 2439
5. Hartwig J F, Cook K S, Hapke M, Incarvito C D, Fan Y B, Webster C E and Hall M B 2005 *J. Am. Chem. Soc.* **127** 2538
6. Hartwig J F 2008 *Nature* **455** 314
7. Periana R A, Bhalla G, Tenn W J, Young K J H, Liu X Y and Ziatdinov V R 2004 *J. Mol. Catal. A-Chem.* **220** 7
8. Crabtree R H 2004 *J. Organomet. Chem.* **689** 4083
9. Davies H M L and Beckwith R E J 2003 *Chem. Rev.* **103** 2861
10. Stahl S S, Labinger J A and Bercaw J E 1998 *Angew. Chem. Int. Ed.* **37** 2180
11. Sen A 1998 *Acc. Chem. Res.* **31** 550
12. Ryabov A D 1990 *Chem. Rev.* **90** 403
13. Houlden C E, Hutchby M, Bailey C D, Ford J G, Tyler S N G, Gagne M R, Lloyd-Jones G C and Booker-Milburn K I 2009 *Angew. Chem., Int. Ed.* **48** 1830
14. Schoenberg A, Bartoleti I and Heck R F 1974 *J. Org. Chem.* **39** 3318
15. Schoenberg A and Heck R F 1974 *J. Org. Chem.* **39** 3327
16. Zhang X H, Geng Z Y, Wang Y C, Hou X F and Wang D M 2012 *J. Mol. Catal. A-Chem.* **363–364** 31
17. Orito K, Horibata A, Nakamura T, Ushito H, Nagasaki H and Tokuda M 2004 *J. Am. Chem. Soc.* **126** 14342
18. Giri R, Maugel N, Li J J, Wang D H, Breazzano S P, Saunders L B and Yu J Q 2007 *J. Am. Chem. Soc.* **129** 3510
19. Whisler M C, MacNeil S, Snieckus V and Beak P 2004 *Angew. Chem. Int. Ed.* **43** 2206
20. Mei T S, Giri R, Maugel N and Yu J Q 2008 *Angew. Chem. Int. Ed.* **47** 5215
21. Alberico D, Scott M E and Lautens M 2007 *Chem. Rev.* **107** 174
22. Giri R, Lam J K and Yu J Q 2010 *J. Am. Chem. Soc.* **132** 686
23. Giri R and Yu J Q 2008 *J. Am. Chem. Soc.* **130** 14082
24. Parr R G and Yang W 1989 *Density-functional theory of atoms and molecules* (New York: Oxford University Press)
25. Becke A D 1993 *J. Chem. Phys.* **98** 5648
26. Frisch M J *et al.* 2004 *Gaussian 03*, Revision E.01 (Wallingford: Gaussian, Inc.)
27. Li Z, Fu Y, Guo Q X and Liu L 2008 *Organometallics* **27** 4043
28. Chung K, Banik S M, Crisci A G D, Pearson D M and Waymouth R M 2013 *J. Am. Chem. Soc.* **135** 7593
29. García-Melchor M, Pacheco M C, Nájera C, Lledós A and Ujaque G 2012 *ACS Catal.* **2** 135
30. Rassolov V A, Ratner M A, Pople J A, Redfern P C and Curtiss L A 2001 *J. Comput. Chem.* **22** 976
31. Andrae D, Haussermann U, Dolg M, Stoll H and Preuss H 1990 *Theor. Chim. Acta* **77** 123
32. Wang X, Hanson J C, Rodriguez J A, Belver C and Fernandez-Garcia M 2005 *J. Chem. Phys.* **122** 154711
33. Gonzalez C and Schlegel H B 1989 *J. Chem. Phys.* **90** 2154
34. Tomasi J and Persico M 1994 *Chem. Rev.* **94** 2027
35. Mineva T, Russo N and Sicilia E 1998 *J. Comput. Chem.* **19** 290